

RESEARCH ARTICLE

Coupling interfaces between hollow carbon dodecahedrons and layered double hydroxides for high-performance rechargeable zinc–air batteries

Jing Zhang^{1,2}, Luo Xu², Yan Lin³, Baojian Xie^{1,2}, Chunjie Li², Tao Hu³,
Ulla Lassi^{3,†}, Ruguang Ma^{2,‡}, Chang Ming Li^{2,§}

¹ School of Physical Science and Technology, Suzhou University of Science and Technology,
Suzhou 215009, China

² School of Materials Science and Engineering, Suzhou University of Science and Technology,
Suzhou 215009, China

³ Research Unit of Sustainable Chemistry, University of Oulu, Oulu 90570, Finland

Corresponding authors. E-mail: [†]ulla.lassi@oulu.fi, [‡]ruguangma@usts.edu.cn, [§]ecmli@usts.edu.cn

Received March 13, 2024; accepted May 9, 2024

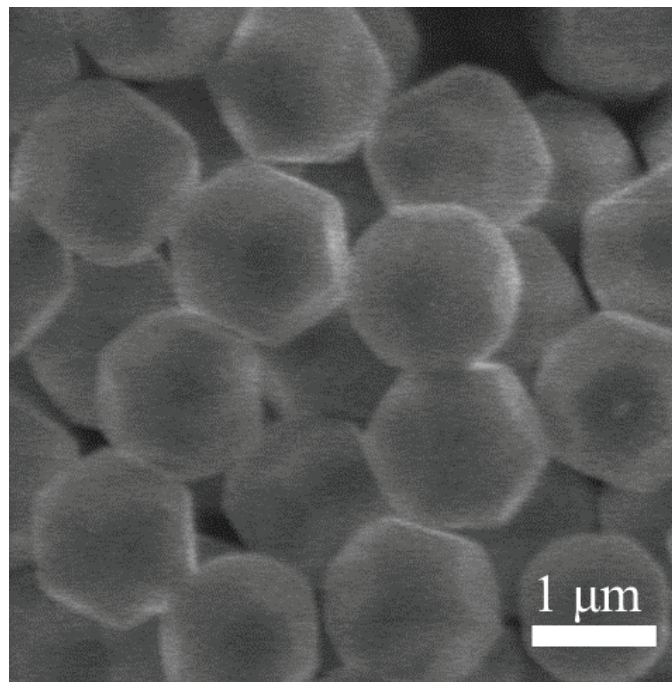
Supporting Information

Fig. S1 SEM image of ZIF-8.

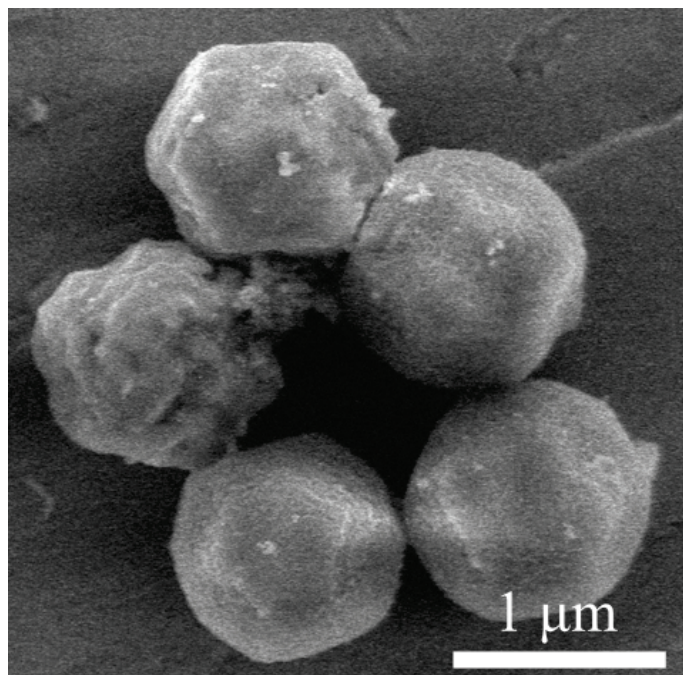


Fig. S2 SEM image of Fe-ZIF-8.

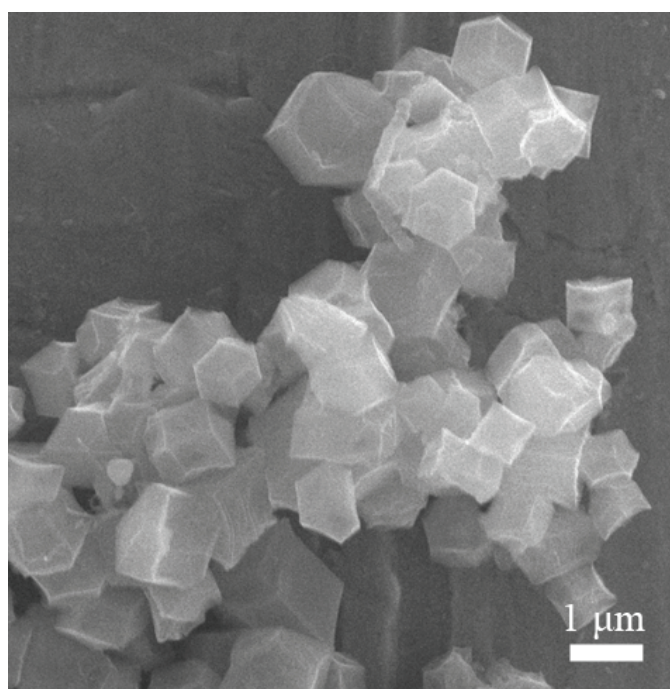


Fig. S3 SEM image of FeNC.

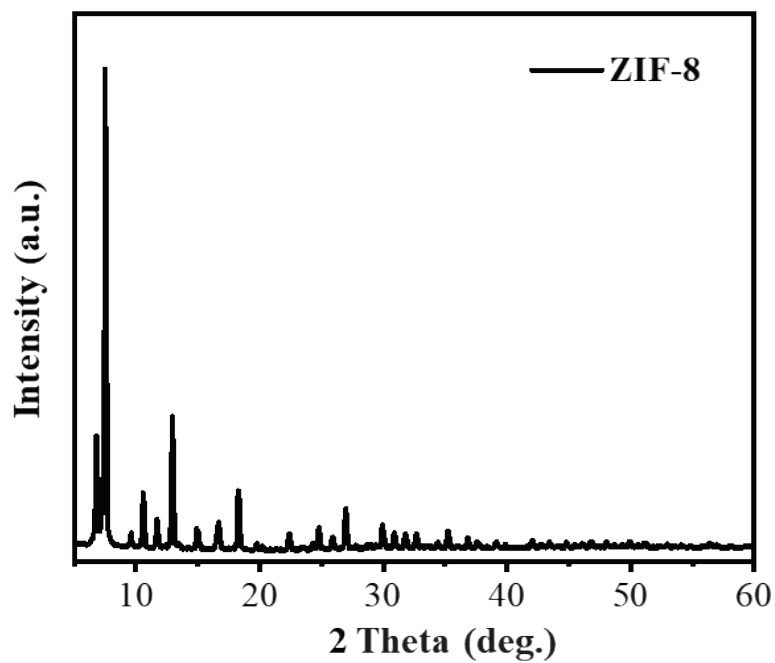


Fig. S4 XRD pattern of ZIF-8.

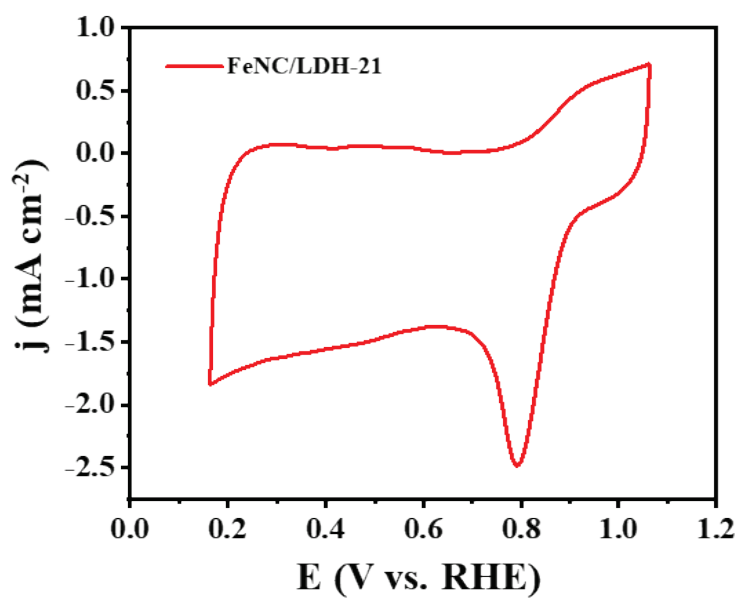


Fig. S5 CV curve of FeNC/LDH-21 in 0.1 M KOH.

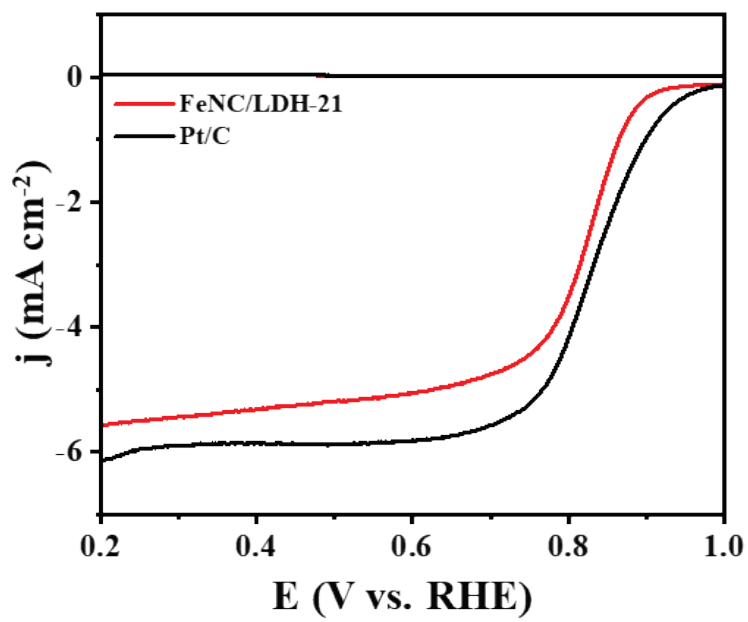


Fig. S6 RRDE polarization curves of FeNC/LDH-21 and Pt/C.

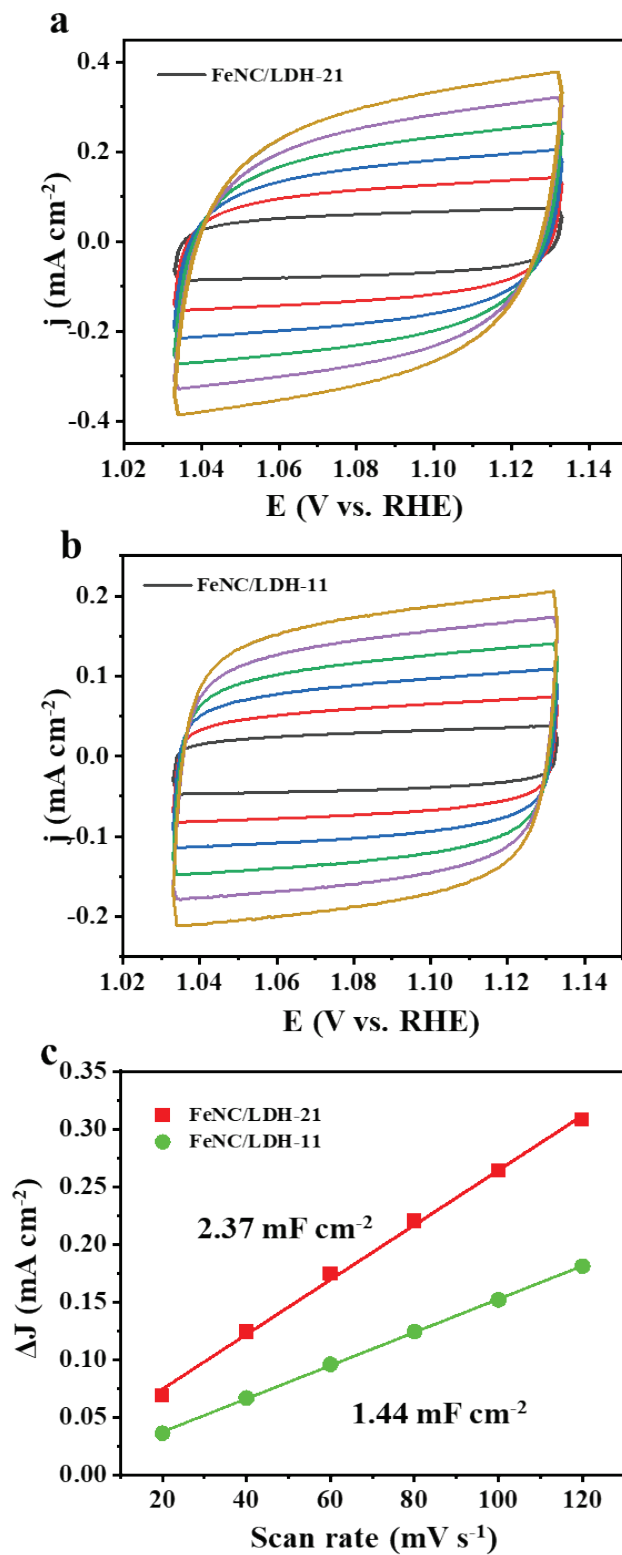


Fig. S7 (a) CV curves of FeNC/LDH-21 and **(b)** FeNC/LDH-11 in the range from 1.03 to 1.13 V at different scan rates. **(c)** Capacitive current density as a function of scan rate derived from the CV curves in (a) and (b).

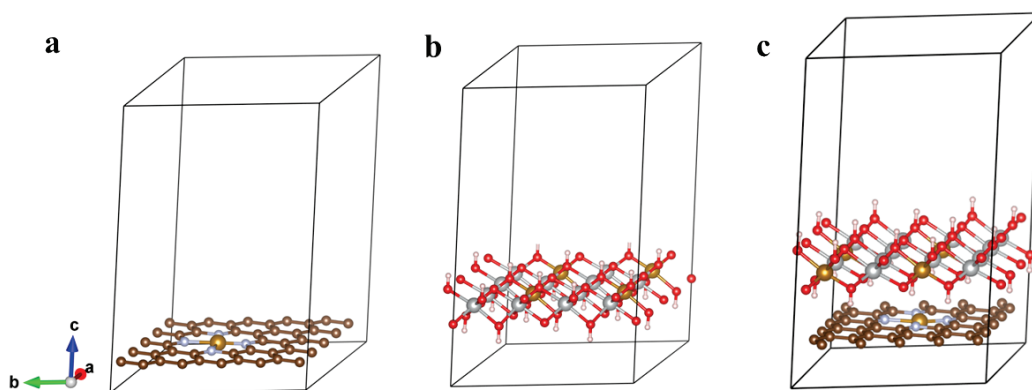


Fig. S8 Structural model of (a) FeNC (b) NiFe LDH and (c) FeNC/LDH heterostructure.

Table S1 Bifunctional performance comparison of the FeNC-LDH-21 electrocatalyst and other reported bifunctional electrocatalysts.

No.	Catalyst	$E_{1/2}$ (V vs. RHE)	η_{10} (V vs. RHE)	ΔE (V)	Ref.
1	FeNC-LDH-21	0.82	1.50	0.68	This work
2	P-NCO/NCN-CF@CC	0.818	1.568	0.75	[1]
3	S-C ₃ N ₄ /CNT	0.83	1.67	0.84	[2]
4	Co _{0.25} Ni _{0.75} @NCNT30	0.84	1.64	0.80	[3]
5	MnO/Co/PGC	0.78	1.54	0.82	[4]
6	MnO ₂ /CNTs	0.80	1.65	0.85	[5]
7	Co-Co ₃ O ₄ @NAC	0.795	1.61	0.815	[6]
8	FeNi ₃ @NC	0.782	1.521	0.74	[7]
9	Co@C-CoNC	0.906	1.638	0.732	[8]
10	FeNC-CoS ₂	0.848	1.608	0.76	[9]
11	CuO/Co ₃ O ₄ @CNTs	0.81	1.59	0.78	[10]
12	A-MnO ₂ /NSPC-2	0.87	1.51	0.64	[11]
13	Co/N-HPCs-800	0.86	1.6	0.74	[12]
14	MoS ₂ -Co@NCNTs-ER	0.85	1.49	0.64	[13]

15	Co ₂ P/Co-NC	0.88	1.60	0.72	[14]
16	LDH@N-CoOx@C	0.84	1.50	0.66	[15]
17	Fe-Co/CNT@MXene-8	0.85	1.59	0.74	[16]
18	CoFe-S@3D-S-NCNT	0.855	1.54	0.71	[17]
19	FeCu-N-HC	0.92	1.64	0.72	[18]
20	FeCo(a)-ACM	0.90	1.60	0.70	[19]
21	FeCo-N-C-700	0.89	1.60	0.71	[20]
22	Fe/Co ₉ S ₈ @NSC	0.82	1.56	0.74	[21]
23	FeCo@CNTs-60	0.95	1.76	0.81	[22]
24	Fe-NC-C ₃ N ₄	0.90	1.535	0.635	[23]
25	Fe-CNTs-rGO	0.82	1.52	0.70	[24]
26	FeCoNi FCNFs	0.92	1.64	0.72	[25]
27	FeCo ₂ Cr@CN	0.703	1.544	0.841	[26]

Table S2 The performance of ZABs by recently reported bifunctional electrocatalysts and FeNC/LDH-21 in this work.

Electrocatalyst	Open-circuit voltage (V)	Maximum power density (mW·cm⁻²)	Specific capacity (mAh·g⁻¹)	Ref.
FeNC/LDH-21	1.51	85	810	This work
F-FeNC	1.49 V	141	760	[27]
Fe-N-C(C)	1.47	131	647.6	[28]
Fe/Fe ₃ C@FeNC	1.414	134.6	856.2	[29]
Fe-Co-N-C	1.48	142.8	806.6	[30]
Hm/ Cy@C-900	1.433	192	766	[31]
Fe-N-C	1.47	111.7	821.8	[32]
Zn-FeNCNs-900	1.50	256	813.3	[33]
HP-Fe-N-C/2	1.513	217	782	[34]
Fe-FeN-C	1.48	206	763	[35]
Fe@FeNC	1.455	179.0	882.8	[36]
FeS/FeNSC	1.50	256.06	807.54	[37]
D-FeNC/MOF	1.603	170	842	[38]
Co@C-CoNC	1.53	162.8	810	[8]
FeSA-FeNC@NSC	1.48	259.88	811.03	[39]
Co ₉ S ₈ /EWPC	1.445	125.1	775.7	[40]
Fe-N-HsGDY	1.49	148	634	[41]
Co-Fe-Ru/PNCS	--	234.3	793	[42]
CoFe@MNC-CNTs	1.50	112.1	813	[43]
Fe-N-C/rGO	1.518	107.1	736.7	[44]

Table S3 The performance of flexible ZABs by recently reported bifunctional electrocatalysts and FeNC/LDH-21 in this work.

Electrocatalyst	Open-circuit voltage (V)	Maximum power density (mW·cm⁻²)	Ref.
FeNC/LDH-21	1.43	32.4	This work
F-FeNC	1.37 V	108	[27]
Fe ₃ C Fe-N-C	1.414	63	[45]
Fe-N-C(C)	1.453	78	[28]
Zn-FeNCNs-900	1.42	128	[33]
HP-Fe-N-C/2	1.476	116	[34]
Fe ₃ Co ₇ -NC	1.51	133	[46]
FeSA-FeNC@NSC	1.4	55.86	[39]
Co ₉ S ₈ /EWPC	1.325	62.4	[40]
CoFe@MNC-CNTs	1.525	--	[43]
Fe-N-C/rGO	1.45	176.1	[44]

References

1. Y. Liu; Z. Jiang; Z.-J. Jiang. Plasma-Assisted Formation of Oxygen Defective NiCoO/NiCoN Heterostructure with Improved ORR/OER Activities for Highly Durable All-Solid-State Zinc-Air Batteries. *Advanced Functional Materials*. 33(35), 2302883 (2023)
2. H. Lei; M. Cui; Y. Huang. S-Doping Promotes Pyridine Nitrogen Conversion and Lattice Defects of Carbon Nitride to Enhance the Performance of Zn–Air Batteries. *ACS Applied Materials & Interfaces*. 14(30), 34793 (2022)
3. A. Kundu; A. Samanta; C. R. Raj. Hierarchical Hollow MOF-Derived Bamboo-like N-doped Carbon Nanotube-Encapsulated $\text{Co}_{0.25}\text{Ni}_{0.75}$ Alloy: An Efficient Bifunctional Oxygen Electrocatalyst for Zinc–Air Battery. *ACS Applied Materials & Interfaces*. 13(26), 30486 (2021)
4. X. F. Lu; Y. Chen; S. Wang; S. Gao; X. W. Lou. Interfacing Manganese Oxide and Cobalt in Porous Graphitic Carbon Polyhedrons Boosts Oxygen Electrocatalysis for Zn–Air Batteries. *Advanced Materials*. 31(39), 1902339 (2019)
5. N. Xu; Q. Nie; L. Luo; C. Yao; Q. Gong; Y. Liu; X.-D. Zhou; J. Qiao. Controllable Hortensia-like MnO_2 Synergized with Carbon Nanotubes as an Efficient Electrocatalyst for Long-Term Metal–Air Batteries. *ACS Applied Materials & Interfaces*. 11(1), 578 (2019)
6. X. Zhong; W. Yi; Y. Qu; L. Zhang; H. Bai; Y. Zhu; J. Wan; S. Chen; M. Yang; L. Huang; M. Gu; H. Pan; B. Xu. Co single-atom anchored on Co_3O_4 and nitrogen-doped active carbon toward bifunctional catalyst for zinc-air batteries. *Applied Catalysis B: Environmental*. 260, 118188 (2020)
7. X. Xie; H. Peng; K. Sun; X. Lei; R. Zhu; Z. Zhang; G. Ma; Z. Lei. Rational construction of FeNi_3/N doped carbon nanotubes for high-performance and reversible oxygen catalysis reaction for rechargeable Zn-air battery. *Chemical Engineering Journal*. 452, 139253 (2023)
8. S. Chandrasekaran; R. Hu; L. Yao; L. Sui; Y. Liu; A. Abdelkader; Y. Li; X. Ren; L. Deng. Mutual Self-Regulation of d-Electrons of Single Atoms and Adjacent Nanoparticles for Bifunctional Oxygen Electrocatalysis and Rechargeable Zinc-Air Batteries. *Nano-Micro Letters*. 15(1), 48 (2023)
9. Y. Mi; W. Wang; Y. Hao; Y. Kang; S. Imhanria; Z. Lei. CoS_2 strongly coupled with porous FeNC as efficient and stable electrocatalyst for rechargeable zinc-air batteries. *Journal of the Taiwan Institute of Chemical Engineers*. 118, 334 (2021)
10. X. Zhang; Q. Liu; Z. Yan; S. Liu; E. Wang. $\text{CuO}/\text{Co}_3\text{O}_4$ heterostructures with carbon nanotubes composites as ORR/OER electrocatalysts for Zn-air batteries. *Journal of Energy Storage*. 66, 107485 (2023)
11. L. Huo; M. Lv; M. Li; X. Ni; J. Guan; J. Liu; S. Mei; Y. Yang; M. Zhu; Q. Feng; P. Geng; J. Hou; N. Huang; W. Liu; X. Y. Kong; Y. Zheng; L. Ye. Amorphous MnO_2 Lamellae Encapsulated Covalent Triazine Polymer-Derived Multi-Heteroatoms-Doped Carbon for ORR/OER Bifunctional Electrocatalysis. *Advanced Materials*. 2024, 2312868 (2024)
12. J. Nie; M. Dong; G. Chen; N. Wang; J. Nie; G. Ma. Biomass-based Hierarchical Porous ORR and OER Bifunctional Catalysts with Strong Stability for Zn-Air

- Batteries. *ACS Sustainable Chemistry & Engineering*. 11(30), 11161 (2023)
13. M. Lv; C. Luo; J. Li; Y. Zhang; Q. Zeng; N. Huang; S. Wang; Y. Zheng; W. Liu; L. Ye. Quasi-Solid-State Flexible Zn–Air Batteries with a Hydrophilic-Treated Co@NCNTs Array Electrocatalyst and PEO–PANa Electrolyte. *ACS Materials Letters*. 5(3), 744 (2023)
 14. X. Liu; J. Wu; Z. Luo; P. Liu; Y. Tian; X. Wang; H. Li. Co₂P-Assisted Atomic Co–N₄ Active Sites with a Tailored Electronic Structure Enabling Efficient ORR/OER for Rechargeable Zn–Air Batteries. *ACS Applied Materials & Interfaces*. 15(7), 9240 (2023)
 15. Y. Hao; Y. Kang; H. Kang; H. Xin; F. Liu; L. Li; W. Wang; Z. Lei. Self-grown layered double hydroxide nanosheets on bimetal-organic frameworks-derived N-doped CoO_x carbon polyhedra for flexible all-solid-state rechargeable Zn-air batteries. *Journal of Power Sources*. 524, 231076 (2022)
 16. C. Zhang; H. Dong; B. Chen; T. Jin; J. Nie; G. Ma. 3D MXene anchored carbon nanotube as bifunctional and durable oxygen catalysts for Zn–air batteries. *Carbon*. 185, 17 (2021)
 17. D. Zhao; L. Zhang; S. Zuo; X. Lv; M. Zhao; P. Sun; X. Sun; T. L. Liu. Developing Superior Hydrophobic 3D Hierarchical Electrocatalysts Embedding Abundant Catalytic Species for High Power Density Zn–Air Battery. *Small*. 19(18), 2206067 (2023)
 18. H. Sun; M. Wang; S. Zhang; S. Liu; X. Shen; T. Qian; X. Niu; J. Xiong; C. Yan. Boosting Oxygen Dissociation over Bimetal Sites to Facilitate Oxygen Reduction Activity of Zinc-Air Battery. *Advanced Functional Materials*. 31(4), 2006533 (2021)
 19. C. Chen; D. Cheng; S. Liu; Z. Wang; M. Hu; K. Zhou. Engineering the multiscale structure of bifunctional oxygen electrocatalyst for highly efficient and ultrastable zinc-air battery. *Energy Storage Materials*. 24, 402 (2020)
 20. X. Duan; S. Ren; N. Pan; M. Zhang; H. Zheng. MOF-derived Fe,Co@N–C bifunctional oxygen electrocatalysts for Zn–air batteries. *Journal of Materials Chemistry A*. 8(18), 9355 (2020)
 21. X. Lei; W. Li; K. Sun; S. Liu; A. Liang; H. Peng; G. Ma. Fe doped Co₉S₈ nanoparticles embedded in N, S co-doped porous carbon as an efficient bifunctional electrocatalyst for rechargeable Zn-air batteries. *Electrochimica Acta*. 476, 143767 (2024)
 22. C. Fang; X. Tang; Q. Yi. Adding Fe/dicyandiamide to Co-MOF to greatly improve its ORR/OER bifunctional electrocatalytic activity. *Applied Catalysis B: Environmental*. 341, 123346 (2024)
 23. C. Chen; S. Zhou; J. Xia; L. Li; X. Qian; F. Yin; G. He; H. Chen. g-C₃N₄ promoted MOF-derived Fe single atoms anchored on N-doped hierarchically porous carbon for high-performance Zn-air batteries. *Journal of Colloid and Interface Science*. 653, 551 (2024)
 24. J. Zhang; C. Li; Y. Zheng; M. Shen; H. Wen; R. Ma. Nickel-iron layered double hydroxides interlinked by N-doped carbon network as bifunctional electrocatalysts for rechargeable zinc-air batteries. *Diamond Relat Mater*. 141, 110596 (2024)

25. X. Meng; Y. Yuan; J. Feng; C. Ma; Y. Sun; J. Zhang; B. Pang; Y. Chen; L. Yu; L. Dong. Design and synthesis of self-supporting FeCoNi- and N-doped carbon fibers/nanotubes as oxygen bifunctional catalysts for solid-state flexible Zn-air batteries. *Chemical Engineering Journal*. 479, 147648 (2024)
26. R. Kumar; S. Kumar; S. G. Chandrappa; N. Goyal; A. Yadav; N. R. Shankar; A. S. Prakash; B. Sahoo. Nitrogen-doped carbon nanostructures embedded with Fe-Co-Cr alloy based nanoparticles as robust electrocatalysts for Zn-air batteries. *Journal of Alloys and Compounds*. 173862 (2024)
27. T. Yang; Y. Chen; M. Tian; X. Liu; F. Zhang; J. Zhang; K. Wang; S. Gao. Engineering the electronic structure of Fe-N/C catalyst via fluorine self-doping for enhanced oxygen reduction reaction in liquid and all-solid-state Zn-air batteries. *Electrochimica Acta*. 443, 141907 (2023)
28. H. Xu; L. Xiao; P. Yang; X. Lu; L. Liu; D. Wang; J. Zhang; M. An. Solvent environment engineering to synthesize FeNC nanocubes with densely Fe-N_x sites as oxygen reduction catalysts for Zn-air battery. *Journal of Colloid and Interface Science*. 638, 242 (2023)
29. N. Huang; W. Dong; Y. Feng; W. Liu; L. Guo; J. Xu; X. Sun. Using dopamine interlayers to construct Fe/Fe₃C@FeNC microspheres of high N-content for bifunctional oxygen electrocatalysts of Zn-air batteries. *Dalton Transactions*. 52(8), 2373 (2023)
30. Q. Zhu; T. Xiang; C. Chen; J. Zhang; Z. Wu; S. Rao; B. Li; J. Yang. Enhancing activity and stability of FeNC catalysts through co incorporation for oxygen reduction reaction. *Journal of Colloid and Interface Science*. 663, 53 (2024)
31. Z. Li; Y. Xie; J. Gao; X. Zhang; J. Zhang; Y. Liu; G. Li. The promotional effect of multiple active sites on Fe-based oxygen reduction electrocatalysts for a zinc-air battery. *Journal of Materials Chemistry A*. 11(48), 265739 (2023)
32. X.-S. Guo; Z.-Y. Huang; X.-W. Qi; L.-P. Si; H. Zhang; H.-Y. Liu. The optimization of iron porphyrin@MOF-5 derived FeNC electrocatalysts for oxygen reduction reaction in zinc-air batteries. *Journal of Electroanalytical Chemistry*. 936, 117381 (2023)
33. Q. Zhou; M. Min; M. Song; S. Cui; N. Ding; M. Wang; S. Lei; C. Xiong; X. Peng. In Situ Construction of Zinc-Mediated Fe, N-Codoped Hollow Carbon Nanocages with Boosted Oxygen Reduction for Zn-Air Batteries. *Small*. 2307943
34. X. Lu; Y. Li; P. Yang; Y. Wan; D. Wang; H. Xu; L. Liu; L. Xiao; R. Li; G. Wang; J. Zhang; M. An; G. Wu. Atomically dispersed Fe-N-C catalyst with densely exposed Fe-N₄ active sites for enhanced oxygen reduction reaction. *Chemical Engineering Journal*. 485, 149529 (2024)
35. X. Lu; Y. Li; D. Dong; Y. Wan; R. Li; L. Xiao; D. Wang; L. Liu; G. Wang; J. Zhang; M. An; P. Yang. Coexisting Fe single atoms and nanoparticles on hierarchically porous carbon for high-efficiency oxygen reduction reaction and Zn-air batteries. *Journal of Colloid and Interface Science*. 653, 654 (2024)
36. W. Dong; W. Liu; Y. Feng; N. Huang. The chemical state of iron species influence on the performance of Fe-N-C bifunctional electrocatalyst for Zn-air batteries. *Nanotechnology*. 35(6), 065402 (2024)

37. J. Chen; B. Huang; R. Cao; L. Li; X. Tang; B. Wu; Y. Wu; T. Hu; K. Yuan; Y. Chen. Steering Local Electronic Configuration of Fe–N–C-Based Coupling Catalysts via Ligand Engineering for Efficient Oxygen Electroreduction. *Advanced Functional Materials*. 33, (4), 2209315 (2023)
38. X. Xu; C. Shu; R. Jin; H. Chen; C. Xu; Y. Liu; L. Sun; C. Guo; H. Chen; W. Liao. Design of nanosheet/nanotube composites of Fe, N-doped carbon for enhanced oxygen reduction in zinc-air batteries. *Electrochimica Acta*. 465, 142986 (2023)
39. W. Zhai; S. Huang; C. Lu; X. Tang; L. Li; B. Huang; T. Hu; K. Yuan; X. Zhuang; Y. Chen. Simultaneously Integrate Iron Single Atom and Nanocluster Triggered Tandem Effect for Boosting Oxygen Electroreduction. *Small*. 18, (15), 2107225 (2022)
40. W. Fang; F. Luo; J. Zhao; H. Dong; J. Zhu; M. Wu. Co₉S₈ nanoparticles embedded in egg white-derived porous carbon as an efficient bifunctional cathode catalyst for Zn–air batteries. *Sustainable Energy & Fuels*. 6(22), 5111 (2022)
41. X. Wang; X. Hu; L. Zheng; Q. Lv; J. He; X. Li; R. Li; T. Lu; C. Huang. The synthesis of MNC₅ active site for electrochemical catalysis. *Nano Energy*. 117, 108919 (2023)
42. Z. Peng; C. Han; C. Huang; Z. Dong; X. Ma. Preventing surface passivation of transition metal nanoparticles in oxygen electrocatalyst to extend the lifespan of Zn-air battery. *Journal of Materials Science & Technology*. 128, 205 (2022)
43. Z. Zhu; Y. Li; X. Li; H. Qiu; L. Fang; L. Zheng; J. Gao; G. Zhu. Bifunctional catalysts of modified doped small-sized ZIF and CNTs with entangled structures. *Diamond Relat Mater*. 140, 110509 (2023)
44. L. Li; Y.-J. Chen; H.-R. Xing; N. Li; J.-W. Xia; X.-Y. Qian; H. Xu; W.-Z. Li; F.-X. Yin; G.-Y. He; H.-Q. Chen. Single-atom Fe-N₅ catalyst for high-performance zinc-air batteries. *Nano Research*. 15(9), 8056 (2022)
45. Y. Chen; X. Kong; Y. Wang; H. Ye; J. Gao; Y. Qiu; S. Wang; W. Zhao; Y. Wang; J. Zhou; Q. Yuan. A binary single atom Fe₃C|FeNC catalyst by an atomic fence evaporation strategy for high performance ORR/OER and flexible Zinc-air battery. *Chemical Engineering Journal*. 454, 140512 (2023)
46. T. Gu; D. Zhang; Y. Yang; C. Peng; D. Xue; C. Zhi; M. Zhu; J. Liu. Dual-Sites Coordination Engineering of Single Atom Catalysts for Full-Temperature Adaptive Flexible Ultralong-Life Solid State Zn–Air Batteries. *Advanced Functional Materials*. 33(8), 2212299 (2023)